

Real-time second-harmonic-generation microscopy based on a 2-GHz repetition rate Ti:sapphire laser

Shi-Wei Chu, Tzu-Ming Liu, and Chi-Kuang Sun

Graduate Institute of Electro-Optical Engineering, National Taiwan University, Taipei, 10617 Taiwan, R.O.C.

Tel: +886-2-23635251 ext. 319. FAX: +886-2-23677467.

sun@cc.ee.ntu.edu.tw

Cheng-Yung Lin and Huai-Jen Tsai

Institute of Fisheries Science, National Taiwan University, Taipei 10617, Taiwan, R.O.C.

Abstract: The problem of weak harmonic generation signal intensity limited by photodamage probability in optical microscopy and spectroscopy could be resolved by increasing the repetition rate of the excitation light source. Here we demonstrate the first photomultiplier-based real-time second-harmonic-generation microscopy taking advantage of the strongly enhanced nonlinear signal from a high-repetition-rate Ti:sapphire laser. We also demonstrate that the photodamage possibility in common biological tissues can be efficiently reduced with this high repetition rate laser at a much higher average power level compared to the commonly used ~80-MHz repetition rate lasers.

©2003 Optical Society of America

OCIS codes: (170.3880) Medical and biological imaging; (170.5810) Scanning microscopy; (170.6900) Three-dimensional microscopy; (190.1900) Diagnostic applications of nonlinear optics

References and links

1. G. Dolino, "Direct observation of ferroelectric domains in TGS with second-harmonic light," *Appl. Phys. Lett.* **22**, 123-124 (1973).
2. J. N. Gannaway and C. J. R. Sheppard, "Second-harmonic imaging in the scanning optical microscope," *Opt. Quantum Electron.* **10**, 435 (1978).
3. Y. R. Shen, "Surface properties probed by 2nd harmonic and sum frequency generation," *Nature* **337**, 519 (1989).
4. C.-K. Sun, S.-W. Chu, S.-P. Tai, S. Keller, U. K. Mishra, and S. P. DenBaars, "Scanning second-harmonic-generation and third-harmonic-generation microscopy of GaN," *Appl. Phys. Lett.* **77**, 2331-2333 (2000).
5. C.-K. Sun, S. W. Chu, S. P. Tai, S. Keller, A. Abare, U. K. Mishra, and S. P. DenBaars, "Mapping Piezoelectric-Field Distribution in Gallium Nitride with Scanning Second-Harmonic Generation Microscopy," *Scanning* **23**, 182 (2001).
6. P. J. Campagnola, M. -D. Wei, A. Lewis, and L. M. Loew, "High resolution nonlinear optical imaging of live cells by second harmonic generation," *Biophys. J.* **77**, 3341-3349 (1999).
7. L. Moreaux, O. Sandre, M. Blanchard-Desce, and J. Mertz, "Membrane imaging by simultaneous second-harmonic generation and two-photon microscopy," *Opt. Lett.* **25**, 320-322 (2000).
8. G. Peleg, A. Lewis, M. Linial, and L. M. Loew, "Nonlinear optical measurement of membrane potential around single molecules at selected cellular sites," *Proc. Natl. Acad. Sci.* **96**, 6700-6704 (1999).
9. I. Freund, M. Deutsch, and A. Sprecher, "Connective Tissue Polarity: Optical Second-harmonic Microscopy, Crossed-beam Summation, and Small-angle Scattering in Rat-tail Tendon," *Biophys. J.* **50**, 693-712 (1986).
10. Y. Guo, P. P. Ho, A. Tirkslunas, F. Liu, and R. R. Alfano, "Optical harmonic generation from animal tissues by the use of picosecond and femtosecond laser pulses," *Opt. Lett.* **22**, 1323-1325 (1997).
11. S.-W. Chu, I.-S. Chen, T.-M. Liu, C.-K. Sun, S.-P. Lee, B.-L. Lin, P.-C. Cheng, M.-X. Kuo, D.-J. Lin, and H.-L. Liu, "Nonlinear bio-photon crystal effects revealed with multi-modal nonlinear microscopy," *J. Microscopy* **208**, 190-200 (2002).

12. S.-W. Chu, I.-S. Chen, T.-M. Liu, B.-L. Lin, P.-C. Cheng, and C.-K. Sun, "Multi-modal Nonlinear Spectral Microscopy Based on a Femtosecond Cr:forsterite Laser," *Opt. Lett.* **26**, 1909-1911 (2001).
13. Y. Guo, H. E. Savage, F. Liu, S. P. Schantz, P. P. Ho, and R. R. Alfano, "Subsurface tumor progression investigated by noninvasive optical second harmonic tomography," *Proc. Natl. Acad. Sci.* **96**, 10854-10856 (1999).
14. W. Denk, J. H. Strickler, and W. W. Webb, "Two photon laser scanning fluorescence microscopy," *Science* **248**, 73 (1990).
15. K. König, T. W. Becker, P. Fischer, I. Riemann, and K.-J. Halhuber, "Pulse-length dependence of cellular response to intense near-infrared laser pulses in multiphoton microscopes," *Opt. Lett.* **24**, 113-115 (1999).
16. A. Vogel, J. Noack, G. Hüttmann, and G. Paltauf, "Femtosecond-laser-produced low-density plasmas in transparent biological media: A tool for the creation of chemical, thermal and thermomechanical effects below the optical breakdown threshold," *Proc. SPIE* **4633A**, 1-15 (2002).
17. R. Shack, B. Bell, D. Hillman, R. Kingston, A. Landesman, R. Shoemaker, D. Vukobratovich, and P.H. Bartels, "Ultrafast laser scanner microscope-first performance test (biological application)," *IEEE International Workshop on Physics and Engineering in Medical Imaging*, **viii + 292**, 49-57 (1982).
18. M. Kobayashi, K. Fujita, T. Kaneko, T. Takamatsu, O. Nakamura, and S. Kawata, "Second-harmonic-generation microscope with a microlens array scanner," *Opt. Lett.* **27**, 1324-1326 (2002).
19. Private communication with OLYMPUS OPTICAL CO., LTD.
20. Gavin D. Reid and Klaas Wynne, "Ultrafast laser technology and spectroscopy" in *Encyclopedia of Analytical Chemistry*, R.A. Meyers ed. (John Wiley & Sons Ltd, Chichester, UK, 2000)

1. Introduction

1.1 SHG microscopy

Second-harmonic-generation (SHG) is beginning to emerge as a powerful contrast mechanism in nonlinear optical microscopy since the first SHG microscopy demonstration in the 1970s [1-2]. SHG microscopy has been widely applied to various studies including material sciences (nonlinear crystals [2], surfaces/interfaces [3], field distribution in semiconductors [4-5]), biological researches (membrane potentials [6-8], tissue polarity [9-10], bio-photonic crystal effect [11-12]) and medical applications (tumor progress [13]). The properties of SHG are such that it can be used as a probe of local anisotropy, of the distribution of molecular hyperpolarizabilities, of phase-matching properties, and of surface plasmon enhanced interactions. Similar to two-photon fluorescence microscopy (2PFM) [14], SHG microscopy provides superior axial resolution due to the quadratic dependence of SHG on the illumination intensity. Nevertheless, no exogenous staining is required with SHG microscopy, preventing the complex and invasive labeling procedures in common fluorescence techniques.

The observation of SHG with sensitivities comparable to that of other mechanisms based on linear optical effects could only be possible with a high input laser power, which was unsuitable for the study of fragile and sensitive specimens such as biological tissues. Hence, SHG imaging found limited applications in scanning microscopy until a way of enhancing the nonlinear interaction could be found. The advent of mode-locked lasers in the 1980s finally provided an adequate light source to exploit the characteristics of nonlinear optical phenomena. The high peak power of short pulses maximizes the second-harmonic intensity for a given average input power while, however, acute photodamage is also induced from this extremely strong optical flux.

1.2 Optical damage with femtosecond pulses

Because of the need of high peak power for efficient nonlinear processes such as SHG, femtosecond laser pulses focused through microscope objectives of high numerical aperture were routinely used. Under such strong optical fields, the local interaction between light and biological specimen could easily result in permanent damage to biological samples. König *et al.* have demonstrated that the loss of cell viability occurred at an average power of ~7-mW for 150-fs pulses (with a 80-MHz repetition rate), corresponding to a peak power of 0.56-kW, a peak intensity of 0.85-TW/cm², or a pulse energy of ~0.1-nJ [15]. In the same study they also verified the nonlinear nature of the optical damage in the femtosecond pulse regime.

From an experimental point of view, the breakdown threshold is defined by the observation of bubble formation at the laser focus [16]. The results of A. Vogel *et al.* showed that multi-photon ionization and free-electron-induced chemical bond breaking, not related to heating or thermoelastic stresses, probably mediate the highly localized ablation of intracellular structures and intranuclear chromosome dissection [16]. In brief, the mechanism of the optical damage induced by infrared femtosecond laser pulses should be dominated by nonlinear optical processes and thus the maximal obtainable SHG power is limited by the strong peak intensity and high pulse energy of a femtosecond laser instead of its average power.

The tradeoff between desired high SHG average intensity and unwanted nonlinear photodamage can be best balanced by increasing the repetition rate of a laser. With identical peak intensity and pulse energy in each pulse, the mean power of emitted SHG will linearly increase with the increase of repetition rate while no nonlinear photodamage will take place if we keep the peak intensity and pulse energy well below the photodamage threshold. While acquiring dynamic images in nonlinear microscopy, pixel dwelling time must be long enough for the detector to collect sufficient photons. As a result, increasing the repetition rate and thus increasing the nonlinear signal intensity can efficiently reduce the pixel dwelling time as well as the acquisition time per frame. Here we demonstrate the first photomultiplier-based real-time SHG microscopy using the combination of a 2-GHz repetition rate femtosecond Ti:sapphire laser and a fast XY galvanometer mirror scanner. In fact, this laser can be coupled with any other fast-scanning technique such as a polygonal mirror [17] or a microlens array [18] to improve the contrast and the acquisition rate of the system. By increasing the repetition rate of the femtosecond laser pulse train, SHG average intensity could be significantly improved due to the higher tolerable average excitation intensity while the probability of nonlinear photodamage is reduced due to the under-threshold peak intensity and pulse energy.

2. Description of the method

Two femtosecond Ti:sapphire lasers with different repetition rates are used as light sources in a home-built SHG scanning microscope to compare the image quality and photodamage possibility. One source is the Tsunami laser from Spectra-Physics with an 82-MHz repetition rate and a ~130-fs pulsewidth, which is now a standard system in most multi-photon applications. The typical average power output of this laser is ~700-mW under 5-W frequency-doubled Nd:YAG excitation, corresponding to an output pulse energy of 8.5-nJ/pulse. Under tightly focusing, say with a 0.5- μm focal spot size, this pulse energy will induce an optical flux density equal to 11-TW/cm², which is strong enough to produce optical breakdown in transparent aqueous media, not to mention living biological specimens. This explains why the maximum average power allowed in most multi-photon biological applications is limited to <10-mW, to keep the peak intensity two orders of magnitude below the nonlinear breakdown threshold in transparent aqueous media. In this femtosecond system, two prism pairs are required to produce a net negative intracavity group velocity dispersion (GVD) as compensation for the positive GVD introduced by the optical components inside cavity and the self-phase modulation in the Ti:sapphire rod. Therefore the length of the resonant cavity cannot be scaled down and the repetition rate is locked around 82-MHz determined by the cavity length. The availability of dispersive mirrors that impose an amount of negative GVD on an optical pulse upon a reflection has made prismatic intracavity elements that need a certain geometrical path length for dispersion control obsolete. The other laser we used for comparison is a Gigajet 30 laser from GigaOptics GmbH, whose laser has a specially designed cavity built on dispersive mirrors that allows pulsed Ti:sapphire laser oscillation with repetition frequencies up to 2-GHz. The corresponding cavity length of only 150-mm features an extremely compact system. This mode-locked mirror-dispersion-controlled Ti:sapphire ring-cavity laser delivers almost perfectly bandwidth-limited 30-fs pulses with a 600-mW average power, corresponding to a pulse energy of 0.3-nJ/pulse, much smaller than the pulse energy of the conventional Ti:sapphire laser with a similar average output power. In our experiments, the pulse of the 2-GHz laser was first stretched to 130-fs by

inserting a 2-cm long sapphire crystal in the external optical path and confirmed with a SHG based autocorrelator. After propagating through the highly dispersive microscope objective (GVD of UplanApo/IR 60X is 2300-fs^2 at 800-nm [19]), the temporal width of the 2-GHz pulses will be less than twice of that of the 82-MHz pulses according to a dispersion calculation [20]. Both lasers were tuned to 810-nm center wavelength.

Our home-built laser scanning SHG microscope is modified from an Olympus FV300 scanning system combined with an Olympus BX51 upright microscope. The laser output was first shaped and collimated by a telescope to avoid power loss at XY galvanometer mirror scanners and to fit the aperture of the focusing objective. The collimated beam was then coupled into the Olympus FV300 scanning system connecting to the Olympus BX51 microscope with an aperture fitting tube lens. Real-time scanning was accomplished through the high-speed galvanometer mirrors inside FV300. The excitation laser pulse was focused onto the biological sample with a spot size close to diffraction limit by high numeral aperture (NA) objectives (ULWD MIR 80X/NA 0.75; or UplanApo/IR 60X water/NA 1.20, Olympus) and the excited forward-emission spectrum was collected using a high-NA oil-immersion condenser. The focused spot sizes for both lasers were measured to be around $0.8\text{-}\mu\text{m}$ (with a corresponding effective spot-size of $0.57\text{-}\mu\text{m}$ for SHG) for the 0.75 NA objective while they were measured to be around $0.5\text{-}\mu\text{m}$ (with a corresponding effective spot-size of $0.35\text{-}\mu\text{m}$ for SHG) for the 1.2 NA objective at a $0.81\text{-}\mu\text{m}$ excitation wavelength. The fundamental NIR beam was removed with an optical filter (Schott BG39) before spectral or intensity measurements. For spectral measurement, the collected visible light was then directed into a monochromator (SpectraPro-150, Roper Scientific) and recorded by a TE-cooled CCD detector (DV42-0E, Andor Technology). For SHG intensity mapping, a photomultiplier tube (PMT, R928P, Hamamatsu), which was synchronized with the galvanometer mirrors, was placed behind an interference filter allowing only 405-nm light passage and was used to record SHG intensity point by point to form a two-dimensional sectioned image.

3. Results

3.1 SHG enhancement

To demonstrate SHG enhancement with the high repetition rate laser, we chose muscle fibers from a sacrificed laboratory mouse as our viewing object. Muscle fibers are known to exhibit strong nonlinear bio-photonic crystal effect and thus provide strong SHG generation [11]. The sarcomeres in the skeletal muscles are composed of crystalline myosin and actin nanofilaments with 40 and 20 nm periods, respectively, falling into the spatial range of strong SHG activity. The SHG emission spectra from a muscle fiber excited by the 82-MHz and 2-GHz Ti:sapphire lasers are shown in Figs. 1(a) and 1(b), respectively. A broader SHG spectrum from the 2-GHz laser can be observed, corresponding to the broader spectral bandwidth of this laser. The incident average power of the 82-MHz and the 2-GHz lasers were 7.7-mW and 200-mW after microscope objective, respectively. The resulting pulse energy are both $\sim 100\text{-pJ}$ on the muscle fibers (peak intensity $\sim 4 \times 10^{10}\text{ W/cm}^2$ for the 82 MHz laser, $\sim 3 \times 10^{10}\text{ W/cm}^2$ for the 2GHz laser), at least two orders of magnitude smaller than the optical nonlinear

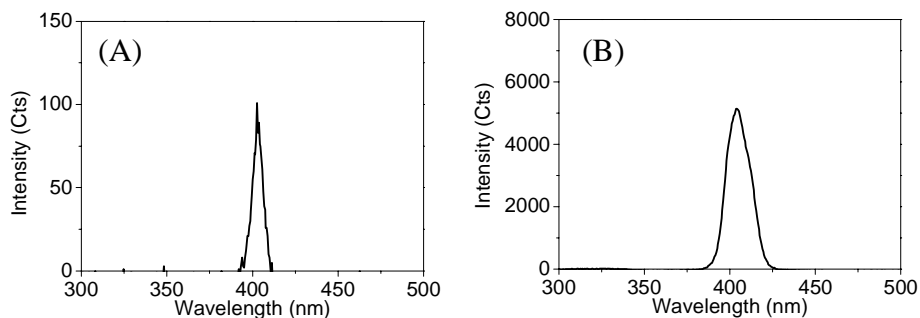


Fig. 1. Nonlinear emission spectra showing the SHG intensity difference from mouse muscle fibers excited by (A) the 82-MHz and (B) the 2-GHz Ti:sapphire lasers.

breakdown threshold in transparent aqueous media [16] and no photodamage was observed throughout the spectroscopic and microscopic measurements under these illumination intensities. Even with a lower peak intensity under the 2GHz laser excitation, almost two orders of magnitude SHG enhancement in muscle fibers was achieved over the generally used 82-MHz one, indicating that this strong enhancement is attributed to the increased repetition rate. Besides in animal tissues, similar SHG enhancement with this high repetition rate laser has also been observed in starch granules.

3.2 Real-time SHG microscopy in zebrafish muscular tissues

With this strongly repetition-rate enhanced SHG signal and lower peak intensity, real-time SHG microscopy becomes realizable. For real-time imaging measurement, we use muscle fibers in live zebrafish larvae. Figure 2 shows the real-time *in vivo* SHG sectioned image series of moving zebrafish muscle fibers taken with the 2-GHz repetition rate Ti:sapphire laser. Individual sarcomeres can be visualized through the *in vivo* SHG images with a bright A-band and a dark I-band as a period. The average power incident on fish muscle fibers was 150-mW, corresponding to a 75-pJ pulse energy and a ~ 0.06 TW/cm² peak intensity with a 60X/NA1.2 water immersion objective. This peak intensity is at least one order of magnitude smaller than the peak intensity threshold for the loss in cell viability demonstrated by König *et al.* [15] while the average incident power, however, is one order of magnitude larger than that in ref. 15. In consequence, no photodamage can be observed while the fast movement of live muscle fibers can be *in vivo* traced in real time. Furthermore, the contraction of muscle fibers inside a vertebrate can also be monitored in real-time through SHG microscopy, which is the first time to our knowledge. According to our result, the maximum contraction of each sarcomere is ~ 100 -nm, which is approximately 5% of its total length. Due to the speed limitation of the galvanometer scanners in FV300, the maximum frame rate is ~ 15 frame per second (fps) for images with 100x512-pixel resolution (4-fps for 512x512-pixel resolution), which was used in Fig. 2.

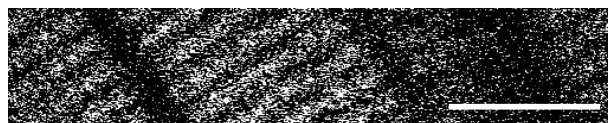


Fig. 2. (705 KB) Real-time (15 fps) SHG microscopic images in live zebrafish muscular tissue with the 2-GHz, 150mW Ti:sapphire laser.

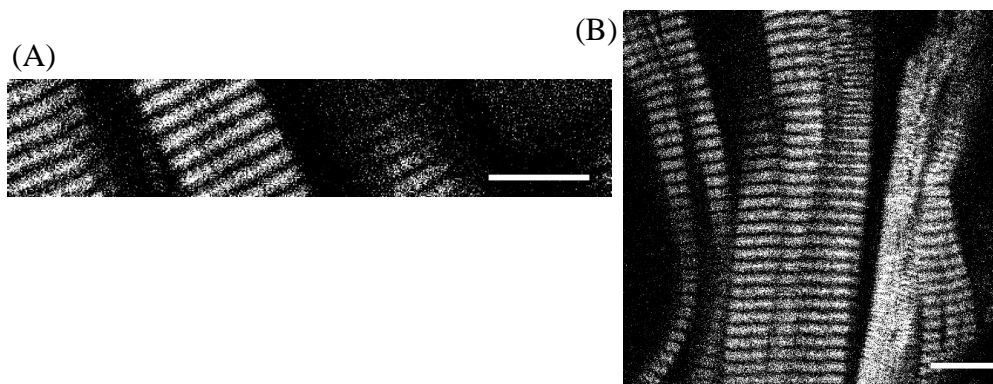


Fig. 3. (1182 KB, 800 KB) Time series of SHG *in vivo* microscopic images in live fish muscle tissue with the 82-MHz, 115mW Ti:sapphire laser showing the dramatic optical damage induced by the excessively strong peak intensity. Scale bar: 10 μ m.

On the other hand, if we used the conventional 82-MHz Ti:sapphire laser with a similar average incident power (115-mW), the corresponding pulse energy and peak intensity will be

as high as 1.4-nJ and 1.6 TW/cm², respectively. Under this extremely strong incident optical field, most biological materials will suffer from violent nonlinear photodamage in company with bubble formations. This destructive process in live zebrafish muscles can be observed in Fig. 3. In both image series, the PMT voltage was decreased a little to avoid signal saturation since the signal intensity is more than 10-fold stronger than that in Fig. 2. This strong signal intensity is of course enough for real-time microscopy applications; only that irreversible strong photodamage will come along. The frame rate in Fig. 3(a) is also 15 fps, adequate to show the dynamics during the breakdown of muscle fibers. It can be observed that the optical damage occurs in less than one second after the onset of laser irradiation. A bubble can be seen clearly after 2-s irradiation and one of the muscle fibers has been totally destroyed. Figure 3(b) shows a larger view on the dramatic nonlinear photodamage process with a slower acquisition rate.



Fig. 4. The SHG microscopic image in fish muscle tissue with the 82-MHz, 8mW Ti:sapphire laser. With the same parameter settings as those in Fig. 2, only noise can be seen. Scale bar: 10 μ m.

If the pulse energy of the 82-MHz laser was attenuated to the safety region (100-pJ) approximately the same as that of the 2-GHz laser in the previous experiments as shown in Fig. 2 (with a higher peak intensity 0.11-TW/cm²), the average power will decay to only ~8-mW, which is a commonly accepted power level when implementing nonlinear microscopy with femtosecond Ti:sapphire lasers. However, with identical measurement parameter settings as in Fig. 2 (including PMT voltage, black and white levels, and frame rate), no SHG from muscle fibers can be observed at all in the scanning image as shown in Fig. 4.

4. Conclusion

We demonstrated an approach to realize the first PMT-based real-time SHG microscopy. The tradeoff between desired high SHG intensity and unwanted nonlinear photodamage can be best balanced by increasing the repetition rate of the applied femtosecond infrared laser. With identical pulse energy and slightly lower peak intensity for pulses from the high repetition rate laser, the mean power of emitted SHG will be strongly enhanced due to high excitation repetition rate while no nonlinear photodamage will take place if we keep the peak intensity well below the damage threshold. While acquiring dynamic images with nonlinear microscopy, pixel dwelling time must be long enough for the detector to collect sufficient photons. As a result, increasing the repetition rate and thus increased nonlinear signal intensity can efficiently reduce the pixel dwelling time as well as the acquisition time per frame. That is to say, by increasing the repetition rate of femtosecond laser pulses, average SHG signal intensity could be significantly improved due to the higher tolerable average fundamental intensity while the probability of nonlinear photodamage is reduced due to the under-threshold peak intensity and pulse energy, resulting in real-time *in vivo* noninvasive SHG microscopy capability. Moreover, this technique can be coupled with any other fast-scanning scheme to improve the contrast and the acquisition rate of the system.

This project is sponsored by National Science Council (NSC-91-2215-E-002-021) and National Health Research Institute (NHRI-EX92-9201EI) of Taiwan, R.O.C. S.-W. Chu would like to acknowledge the generous support from MediaTek Incorporation.